The HKU Scholars Hub   The University of Hong Kong   香港大學學術庫

Title	**Mitigating Voltage and Frequency Fluctuation in Microgrids Using Electric Springs**
Author(s)	**Chen, X; Hou, Y; Tan, SC; Lee, CK; Hui, SYR**
Citation	**IEEE Transactions on Smart Grid, 2015, v. 6 n. 2, p. 508-515**
Issued Date	**2015**
URL	**http://hdl.handle.net/10722/209305**
Rights	**Creative Commons: Attribution 3.0 Hong Kong License**

Mitigating Voltage and Frequency Fluctuation in Microgrids Using Electric Springs

Xia Chen, *Member, IEEE*, Yunhe Hou, *Member, IEEE*, Siew-Chong Tan, *Senior Member, IEEE*,
Chi-Kwan Lee, *Senior Member, IEEE*, and Shu Yuen Ron Hui, *Fellow, IEEE*

Abstract—Voltage and frequency fluctuation associated with renewable integration have been well identified by power system operators and planners. At the microgrid level, a novel device for the implementation of dynamic load response, which is known as the electric springs (ES), has been developed for mitigating both active and reactive power imbalances. In this paper, a comprehensive control strategy is proposed for ES to participate in both voltage and frequency response control. It adopts the phase angle and amplitude control which respectively adjust the active power and the reactive power of the system. The proposed control strategy is validated using a model established with power system computer aided design/electro-magnetic transient in dc system. Results from the case studies show that with appropriate setting and operating strategy, ES can mitigate the voltage and frequency fluctuation caused by wind speed fluctuation, load fluctuation, and generator tripping wherever it is installed in the microgrid.

Index Terms—Control, electric springs (ES), frequency, microgrids, voltage, wind power.

I. INTRODUCTION

DUE TO the energy crisis and environmental concerns, penetration of renewable energy has been increasing dramatically. Renewables can be utilized in large scale, i.e., large wind farms connected with transmission systems, or in small scale, i.e., wind turbines connected to microgrids. At all levels, variability and uncertainty associated with renewable energy sources, such as wind power and solar power, can significantly challenge the operating methodology of traditional power systems [1].

In microgrids, the major challenges of adopting small-scale wind generation are twofold. Firstly, the variation of active

power and reactive power resulting from the wind speed fluctuation will introduce a change in the voltage drop along the power line. This in turn induces a nonnegligible bus voltage variation which may exceed the required power supply limits [2], [3]. The voltage variation may cause serious problem for critical loads, which demand a high-quality voltage supply. Secondly, a large deviation between the supply and the demand due to a fluctuation in the wind power may result in unexpected frequency fluctuation in microgrid systems [4]. Such challenges are well known and some relevant research handling these issues has been reported in [5]–[7].

For microgrids, different measures have been developed to alleviate the negative effects of the voltage disturbance and to mitigate the power quality problems [8], [9]. To solve the voltage dip and swell problems caused by renewable energy fluctuation, static series compensators (SSC), or dynamic voltage restorers (DVR), are introduced to inject a compensating series voltage into the system. In terms of voltage support, these devices are costly and demand complicated protection system due to the utilization in the transmission level compared to the electric springs (ES) application in the distribution with a lower voltage level [10].

For another critical problem in a microgrid, i.e., frequency, some control schemes have been proposed to maintain it within an acceptable region. Generally, these schemes based on the idea that a power reserve bank is provided to smooth the possible power deviations [11]. These methods may lose their effectiveness when a large fluctuating power deviation exceeds the preset power reserve bank [12]. Load shedding has to be employed as the last action in the traditional power systems [13]. Recently, with the development of the energy storage system (ESS), it provides a promising solution for regulating of the wind farm fluctuation [14], [15]. Until now, the cost of the required ESS is very high if the wind power output variation is considerable large [16], [17].

In the context of smart grids, dynamic load response is well identified as an efficient method for mitigating deviations of voltage and frequency, not only for transmission systems, but also for microgrids [18], [19]. Recently, the concept of ES has been proposed as a simple and effective solution for achieving grid voltage stabilization and active power factor compensation at the distribution level [20], [21]. With this solution, ES is connected in series with a noncritical load to become a smart load. The ES possesses an automatic mechanism of regulating the power flow of the noncritical loads to provide the required voltage support across the distribution grid. Therefore, the ES

Fig. 1.   Configuration of an ES.
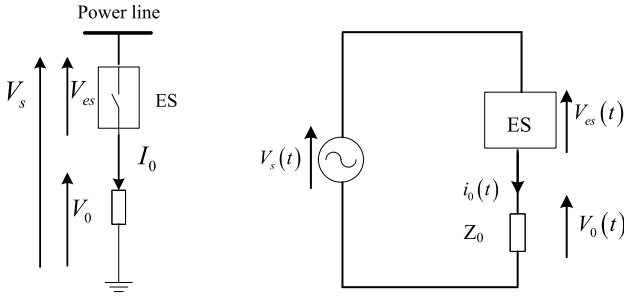

Fig. 2.   Phasor diagram of ES.

Fig. 3.   Circuit diagram of the ES.

operates only at a portion of the voltage instead of the full voltage range of the utilization level [21]. The advantage lies in that the ES contributes only a fraction of the power change and relies heavily on the series noncritical load for shaping the power flow. Hence, for buffering the same power variation, the storage capacity requirement of ES is much smaller than that of the ESS [22]. Also, compared to the SSC that are usually applied at the high-voltage transmission level, an output coupling transformer would be needed in the SSC for voltage conversion [10], whereas no such requirement is needed for the ES. Furthermore, despite the fact that the application of ES at the distribution level of standard power system has been found promising [20]–[22], there has not been any report on the application of ES in a microgrid system.

   In view of this, the objective of this paper is to report the study on the utilization of ES for maintaining the voltage and frequency stability of a nine-bus microgrid system comprising standard power generators and a variable and uncertain power supply in the form of wind energy. Interestingly, this is the first time that the ES is applied for frequency stabilization in addition to their original purpose of the line voltage stabilization. In the following, the operating principle of the ES is firstly analyzed for both the active and reactive power compensations. Then, based on the established mathematical model of the ES, the required control strategy for performing both the line voltage regulation and the load demand control is introduced. Then, simulation results and discussion are presented. Finally, the conclusion is covered.

II. System Configuration and Modeling

A. ES Configuration

   Borrowing the concept of the mechanical spring, the ES has the following functions: 1) provide the electric voltage support; 2) store electric energy; and 3) damp electric oscillations [20]. The configuration of an ES is shown in Fig. 1. The output of the ES is serially connected to a noncritical load to form a smart load. The noncritical load can be a single or a group of electric loads which can tolerate some degrees of voltage variation without causing significant inconvenience to the user.

B. Operational Principle

   The vectorial sum of the noncritical load voltage V_o and the compensation voltage V_{es} is equal to the supply voltage V_s. V_o can be boosted or suppressed by V_{es} which is generated
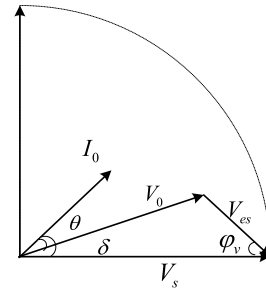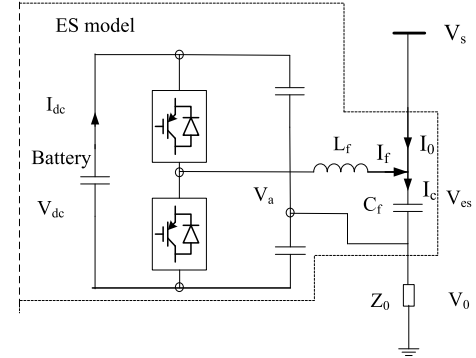
by the ES. Consequently, the power consumption of the noncritical load can be controlled. Fig. 2 shows a phasor diagram of the operation mode of which ES provides the voltage boost function. The ES acts as a series compensator which could provide a variable ac voltage that changes the voltage of the load Z_0, thus changing the power flowing to the load even though the line voltage V_s and the load Z_0 are unchanged.

   The ES can, in principle, perform active and/or reactive power control. For instance, the change of compensation voltage V_{es} can simultaneously provide reactive power compensation to the power system when the voltage V_{es} is controlled in quadrature with the load current I_o. Meanwhile, the active power consumption can be performed when a battery is equipped at the dc side. As far as the charging and discharging of the battery is concerned, during the normal condition, this problem could be avoided. It is assumed that the battery operates in an ideal mode and has good charge/discharge characteristics in this paper. Actually, the batteries can be replaced by other types of bidirectional dc voltage source or a dc/ac bidirectional power converter of which the ac side is connected to the power grid.

III. Control Strategy

   The ES may be implemented using a half-bridge single-phase inverter with an inductor capacitor (LC) output filter for eliminating the high-frequency pulse width modulation (PWM) signal as shown in Fig. 3. The protection of the capacitor in this configuration should be considered with the elaborate design of LC filter. The ES output is connected in series with the grid and also to the load and it can produce either an active ($\pm P_{es}$) and/or reactive power ($\pm jQ_{es}$) difference between the power source and the load. At steady state,

the power relationship between the grid, the load and the ES could be obtained as follows:

$$\begin{cases} P_s = P_0 \pm P_{es} \\ Q_s = Q_0 \pm Q_{es}. \end{cases} \tag{1}$$

The ES power, the load power and the power source are expressed below

$$\begin{cases} P_{es} = |V_{es}| \times |I_0| \cos(\delta + \varphi_v) \\ Q_{es} = |V_{es}| \times |I_0| \sin(\delta + \varphi_v) \end{cases} \tag{2}$$

$$\begin{cases} P_0 = |V_0| \times |I_0| \cos\theta \\ Q_0 = |V_0| \times |I_0| \sin\theta \end{cases} \tag{3}$$

$$\begin{cases} P_s = |V_s| \times |I_0| \cos\delta \\ Q_s = |V_s| \times |I_0| \sin\delta \end{cases} \tag{4}$$

where φ_v is the phase angle between the ES and power supply voltage, δ and θ are the power factor angle of the power supply and load, respectively.

From (1)–(4), the load power can be calculated as shown in

$$\begin{cases} P_0 = |V_s| \times |I_0| \cos\delta - |V_{es}| \times |I_0| \cos(\delta + \varphi_v) \\ Q_0 = |V_s| \times |I_0| \sin\delta - |V_{es}| \times |I_0| \sin(\delta + \varphi_v). \end{cases} \tag{5}$$

In [21], it is concluded that a change in the RMS value of the ES voltage $|V_{es}|$ and the displacement angle of ES voltage φ_v may simultaneously affect both the active and reactive power compensations. ES can provide active power to the grid and to support the frequency control to reduce any sudden, large load-generation imbalance.

The average model for the half-bridge inverter is written as follows:

$$\begin{cases} V_s - V_{es} - Z_0 I_0 = 0 \\ I_0 + I_f = I_c \\ I_c = C_f \dfrac{dV_{es}}{dt} \end{cases} \tag{6}$$

$$\begin{cases} L_f \dfrac{dI_f}{dt} = V_a - V_{es} \\ V_a = \dfrac{V_{dc}}{2} m \end{cases} \tag{7}$$

where L_f and C_f denote the filter inductance and capacitance, respectively, V_{dc} is the dc-link voltage of the inverter, and V_a is the output ac voltage of the inverter.

The modulation index can be written as

$$m = \frac{(V_{sref} - V_s)}{V_{tri}} G_c(t) \tag{8}$$

where $G_c(t)$ is the compensating function; V_{tri} is the amplitude of the PWM triangular carrier; V_{sref} is determined according to the voltage requirement by the critical load, and the rated voltage is usually chosen.

The state space model of the ES is

$$\begin{bmatrix} \dot{V}_{es} \\ \dot{I}_f \end{bmatrix} = \begin{bmatrix} -\frac{1}{Z_0 C_f} & \frac{1}{C_f} \\ -\frac{1}{L_f} & 0 \end{bmatrix} \begin{bmatrix} V_{es} \\ I_f \end{bmatrix} + \begin{bmatrix} 0 \\ \frac{V_{dc}}{2L_f} \end{bmatrix}$$
$$\times \frac{(V_{sref} - V_s)}{V_{tri}} G_c(t) + \begin{bmatrix} \frac{V_s}{Z_0 C_f} \\ 0 \end{bmatrix}. \tag{9}$$

The average linearized model of the ES is shown in Fig. 4.

The control of the ES is different from the traditional SSC using output-voltage control method. With the "input-voltage control" mechanism, an ES regulates the line
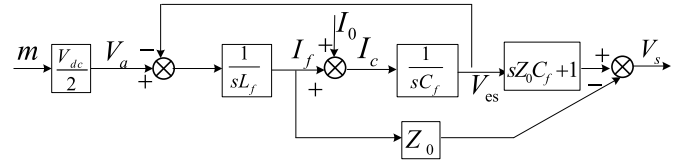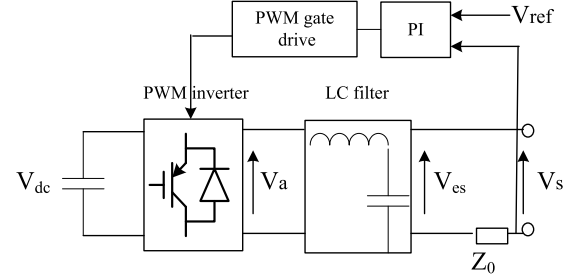

Fig. 4. Average linear model of ES.

Fig. 5. ES with voltage control loop.

voltage V_s by controlling the power flow to the noncritical load and allows the noncritical load voltage V_o to fluctuate dynamically. The modulation index m can be obtained from the control of the line voltage V_s given by (8). As illustrated in Fig. 5, by controlling the m of the PWM inverter, high-quality PWM voltage waveform at the line frequency can be generated. With the use of the low-pass filter, a sinusoidal voltage (V_{es}) with the controllable magnitude by adjusting the m obtained from the ac voltage controller, can be generated as the output of the LC filter. The reactive power may be directly controlled by varying the amplitude of the compensation voltage V_{es} across the filter capacitor of the ES.

The input power equation of the dc-link of the inverter is

$$P_{dc} = V_{dc} I_{dc} = V_{dc} \times C \frac{dV_{dc}}{dt} = \frac{1}{2} C \frac{dV_{dc}^2}{dt}. \tag{10}$$

By assuming an ideal lossless power inverter, the ac output power and the dc input power of the inverter have the following relationship:

$$P_{dc} = P_{es} = P_s - P_0. \tag{11}$$

The ac side power fluctuation may result in the dc-link voltage variation. By controlling the dc-link voltage to be constant, the power balance between the ac and dc link is maintained. At the initial stage, the dc-link capacitor is charged to establish a constant dc voltage. A power fluctuation at the terminal bus results in an error in the dc-link voltage. The dc voltage controller adjusts the phase angle to ensure that the power is balanced between the dc side and ac side of the inverter.

By adjusting the power flow in the ES branch, the active power will be controlled and thus the frequency in the microgrid will be affected. A simplified control block diagram of the ES is shown in Fig. 6. It is important to note that an ES requires two closed-loop controllers to operate. The active power is controlled by the shift angle difference between the angle δ_1 measured by the single phase-locked loop (SPLL) and the angle δ_2 generated by the controller. A classical voltage proportional-integral controller is adopted to maintain the dc-link voltage and the ac line voltage to be constant. In this
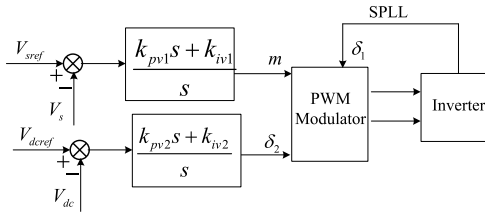
Fig. 6.   Overall control scheme for ES.

Fig. 7.   Nine-bus system.

feedback mechanism, the amplitude and shift angle of the modulation signal are respectively obtained from the compensated line voltage and dc-link voltage errors. The signal *m* is then compared with the reference triangular wave to generate the trigger signal for the on/off of the switch.

For the single-phase system, since only one voltage component can be obtained at any moment, the amplitude and phase angle are not simultaneously available [23]. Time delay is present in sensing the amplitude and phase angle. A PLL composed of a phase detector, a filter, and a voltage-controlled oscillator is utilized to obtain the phase angle information. The structure of the SPLL adopted here is given in the Appendix.

To maintain the regulation of the line voltage, the ES voltage and load voltage can be adjusted accordingly. Simultaneously, the noncritical load power is instantaneously shaped to follow the available power generated by the power system. This is a new demand-side management method that can satisfy the new control paradigm of enabling the load demand to follow the power generation.

For the doubly-fed-induction-generator-based wind turbine control, the wind turbines are operated in the maximum power tracking mode. This operation mode will not reserve any generation margin for frequency response control [24].

The maximum power obtained from a given wind speed is commonly expressed by the following equation [25]:

$$P_{\text{mec}} = \frac{1}{2} C_p \left(\lambda, \beta \right) \pi R^2 \rho v_w^3 \tag{12}$$

where P_{mec} is the mechanical power extracted from the wind, ρ is the air density in kg/m^3, R is the turbine radius in m, v_w is the wind speed in m/s, and $C_p(\lambda, \beta)$ is the aerodynamic power coefficient, which is dependent on both the blade pitch angle β in degrees and the tip speed ratio λ. The tip speed ratio λ is given by

$$\lambda = \frac{\omega_r R}{v_w} \tag{13}$$

where ω_r denotes the turbine rotor speed.

IV. CASE STUDIES

The objective of this paper is to investigate the dynamic behavior of a microgrid system with the ES in enhancing the frequency response and maintaining the line voltage level in the presence of the renewable variability. The ES can operate at various possible types of power compensation. Here, the applications of active power and reactive power compensations by the ES in coping with the frequency control and the line voltage regulation of the microgrid are investigated. A nine-bus system as shown in Fig. 7 is employed in the case
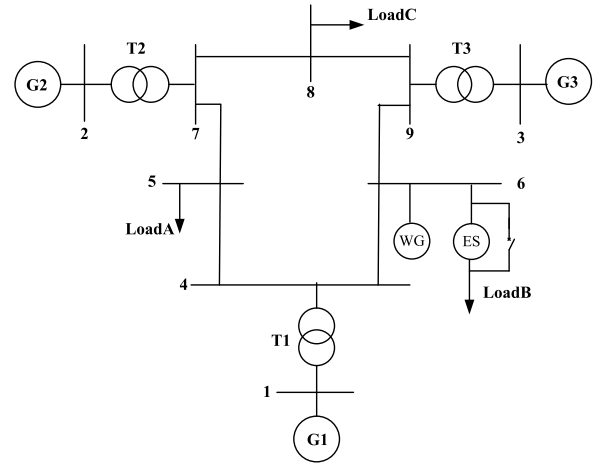
studies. The voltage level for the system is 35 kV and the rated power for the generation 1 (G1), generation 2 (G2), and generation 3 (G3) are 8 MVA, 6 MVA, and 4 MVA, respectively. The base value for active power is 1 MW. Each generator is equipped with a governor. The governors are provided with the speed-droop control to share the load change and participate in the primary frequency control. The ES is installed in series with the load in three-phase connection without the utilization of the transformer. The model of the system is established with power system computer aided design/electro-magnetic transient in dc system. The load on bus 5 is 4.167 + j1.667 MVA, the load on bus 6 is 3 + j1 MVA, and the load on bus 8 is 3.333 + j1.167 MVA. Both the ES and the wind turbine are installed at bus 6.

A. Case 1—Wind Speed Variation

In case study 1, the effect of the variable wind speed on the microgrid with and without the ES is investigated. The ES is located at the same bus with that of the wind turbine. Here, the wind speed increases from 18 to 21 m/s at 6 s. The gust wind lasts for 6 s. The output active power of the wind turbine varies resulting from the gust wind as shown in Fig. 8(a). The three generators respond accordingly and adjust the corresponding output active power in Fig. 8(b). ES is activated in the whole simulation process. The frequency response resulting from the power imbalance is compared in the case of with and without ES as shown in Fig. 8(c). With the ES outputting active power as shown in Fig. 8(d), the frequency peak and nadir due to the gust wind is improved by about 0.2 Hz as compared to the case without the ES.

The voltage and power of the load in series with the ES are regulated as shown in Fig. 9(a) and (b). With the aid of an ES controller, the voltage across the load increases, and thus the power consumed by the load changes following the wind power. The bus voltage can be controlled to maintain almost constant in Fig. 9(c). The voltage amplitude is reduced about 0.01 p.u., and the voltage fluctuation is mitigated with ES outputting reactive power as shown in Fig. 9(d). It should be noted that the generators operate in droop mode. The output powers of generators always remain proportional to their ratings. The primary control is conducted to obtain a proper power-sharing
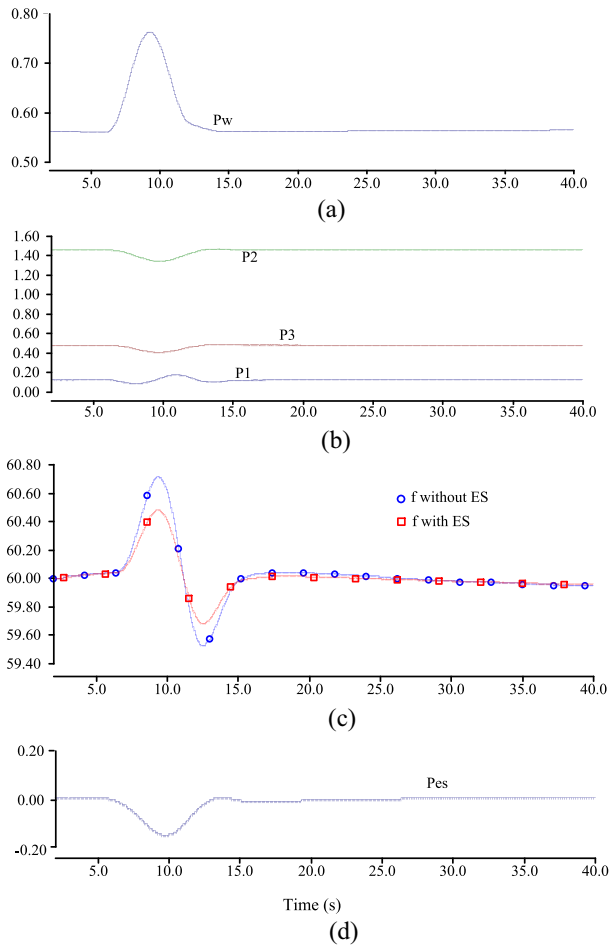
Fig. 8.   (a) Output power of wind turbine (p.u.). (b) Generators output active power (p.u.). (c) Frequency response to wind power variation (Hz). (d) ES active power.

Fig. 9.   (a) Load voltage, (b) load power, and (c) voltage on bus 6 (p.u.). (d) ES reactive power.

between the generators. In Fig. 8(c), the gust wind starts from 6 s and lasts for 6 s. That is, at 6 s, the frequency rises due to the increase power. Meanwhile, the generators begin the primary frequency adjustment to prevent the frequency increase. At 12 s, due to the slow pitch angle adjustment, the output power of the wind turbine keeps decreasing, resulting in the continuous frequency decrease. The primary frequency regulation will last for several seconds until the frequency settles into the steady state. The short-time fluctuation of the wind turbine output power as well as the delay in the power sharing, results in a slow frequency recovery of the system. It can be observed that the capability of the ES in supporting the line voltage and in dynamic balancing the wind power and the load power is demonstrated.

B. Case 2—Load Variation

In case study 2, the effect of load change on the microgrid with and without the ES is investigated. Here, the load on bus 6 steps up to 4 MW at 6 s and then comes back to 3 MW at 10 s. A bypass switch is installed in parallel to the inverter as shown in Fig. 7. The bypass switch keeps close during the normal operation. When the load variation occurs at 6 s, it is set to open at 6.01 s to activate the ES as soon as possible in the simulation and close at 10.01 s once the
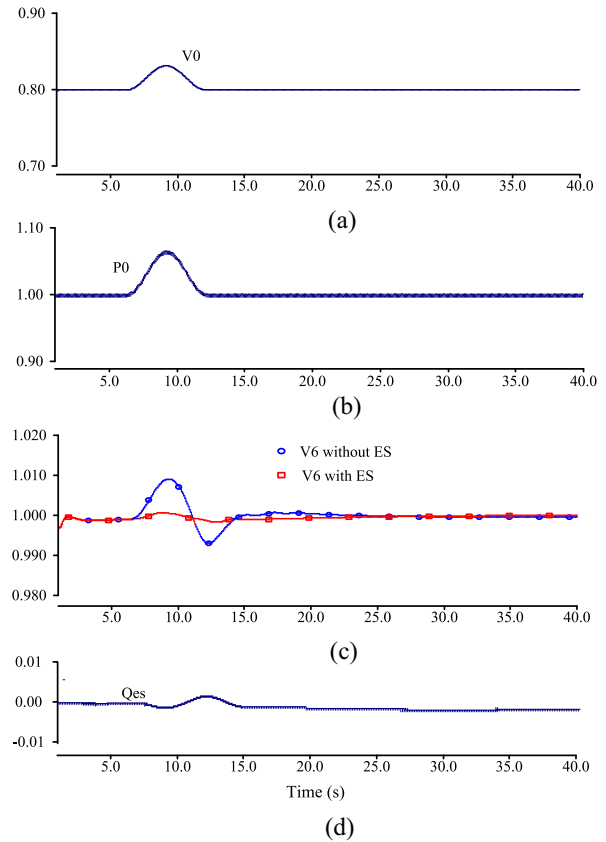
load variation disappears. As shown in Fig. 10, the bus voltage is tightly regulated by the ES to maintain at 1 p.u. during the load variation. With the ES, the frequency nadir occurs at 8 s and is enhanced from 59.6 (without the ES) to 59.8 Hz. Moreover, with the ES active power support by controlling the dc-link voltage at 40 kV, the settling time of the frequency is much shorter than that without the ES as shown in Fig. 10(a). Fig. 10(b) shows the voltage waveform of the ES during the load change. It is shown that ES does provide the voltage support to prevent the voltage dip on bus 6. Fig. 10(c) shows the line voltage on bus 6 being tightly regulated at 1% deviation during the load variation. From this paper, it is shown that the voltage and frequency fluctuation caused by the load variation could be mitigated by the ES through active and reactive power compensation as shown in Fig. 10(d) and (e).

C. Case 3—Generator Tripping

In this case study, the effect of a generator trip on the microgrid with and without the ES is investigated. Here, the wind turbine is not included and the same control strategy as that of cases 1 and 2 is implemented. The total generation of the system is 10.45 MW and the total load demand is 10.4 MW. There is about 0.05 MW power losses in the lines. At 6 s, the G3 is tripped and the lost power is about 2.8 MW as shown in Fig. 11(a). Adopting the conventional load shedding approach, the under-frequency relay is employed to operate after the frequency falls below 58.5 Hz. The shedding of a 3 MW load
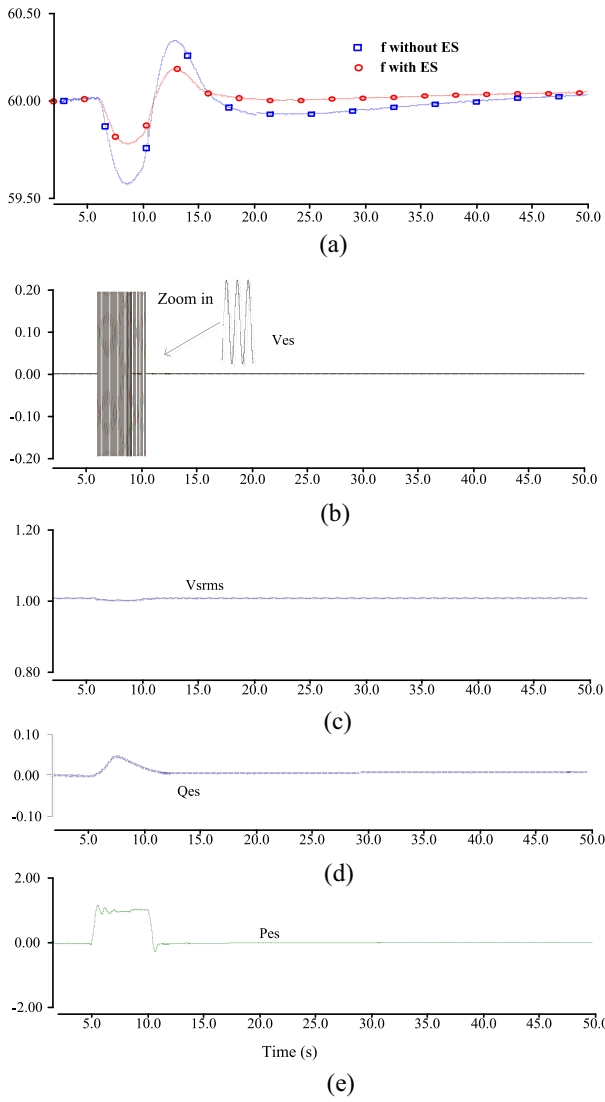
Fig. 10.   (a) Frequency response to load variation (Hz). (b) ES voltage (p.u.). (c) Voltage on bus 6 (p.u.). (d) ES active power. (e) ES reactive power.

Fig. 11.   (a) Generator active power (p.u.). (b) Frequency response to generator tripping (Hz). (c) ES output active power.
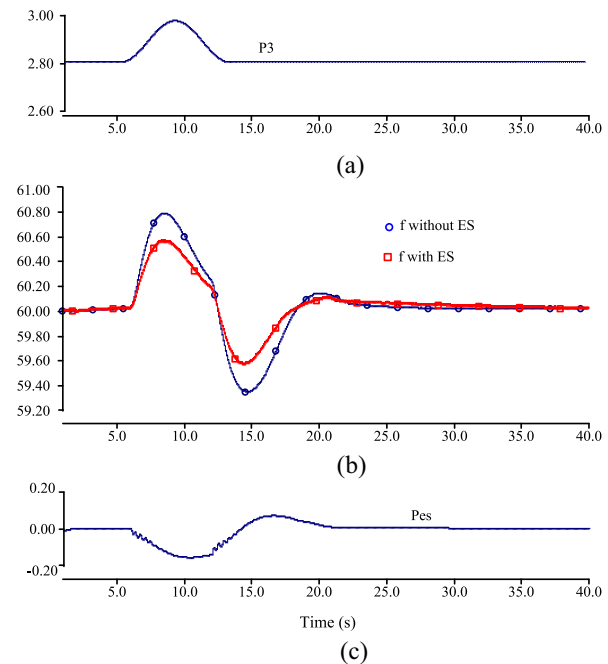
Fig. 12.   (a) Wind turbine output active power (p.u.). (b) Frequency response to wind speed variation (Hz). (c) ES output active power.

brings the system frequency back to 59.5 Hz [see Fig. 11(b)]. However, if the ES is controlled to inject 1 MW power shown in Fig. 11(c) while only 2 MW noncritical load needs shedding when the generator trips, a faster frequency recovery is achieved, as depicted in Fig. 11(b). Moreover, with the ES, the frequency nadir is enhanced from 56.3 (without using ES) to 58 Hz. The frequency can be restored to above 59.5 Hz and the steady-state frequency deviation is slightly improved. Compared to the conventional load shedding, the ES scheme avoids more critical loads shedding from the system and therefore, the power supply reliability for the critical loads could be enhanced.

From these case studies, it is verified that the ES can support the frequency response in a microgrid system in addition to its conventional purpose of regulating line voltage. The effectiveness of both the frequency control and line voltage regulation functions in the microgrid is demonstrated in the cases of power (wind speed) variation, load variation, and generator tripping.

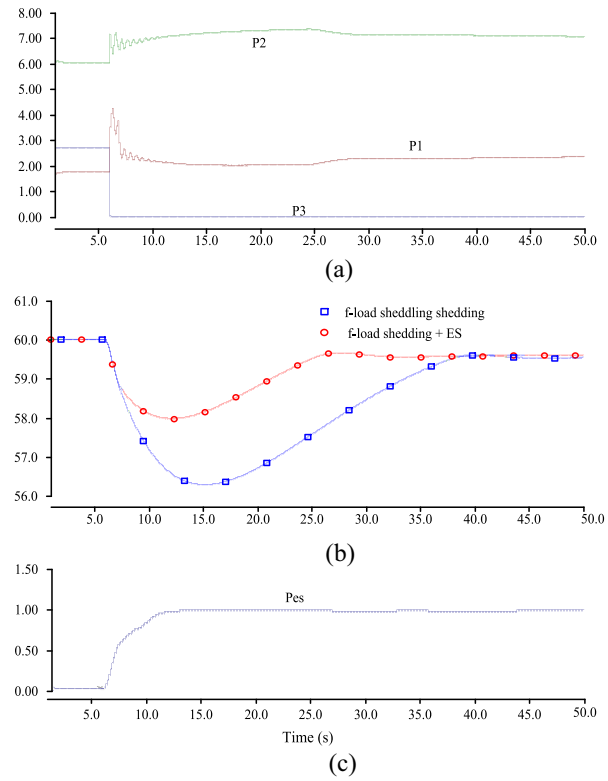### D. Case 4—ES Located at the Different Bus With Wind Turbine

To verify the effectiveness of ES in improving the frequency response when it is installed on the different bus with the wind turbine, the G2 is substituted by the wind turbine while

the ES is still located at the bus 6 without the wind turbine shown in case 1. The wind speed variation is implemented to generate the same power deviation with that in case 1, about 0.2 MW in Fig. 12(a). The wind turbine is not involved in the primary frequency control. The frequency rise is caused by the wind power increase despite of the limited primary frequency control of the remaining generators. Then the ES responds to the frequency variation by absorbing the active power to suppress the frequency rise and accelerate the frequency recovery as shown in Fig. 12(b) and (c). The over frequency is reduced and the under frequency is enhanced about 0.2 Hz, respectively. It can be observed that when the ES is located far away from wind turbine, ES could also improve the frequency response by contributing the active power to the grid. From the simulation results in cases 1 and 4, it can be observed that the frequency variation could be suppressed slightly when ES is located close to the variable and uncertain renewable power source. The frequency deviation has been reduced about 0.1 Hz in case 1 compared to the frequency peak/nadir in case 4 for the sake of less power loss. Wherever it is installed in the microgrid, the problem brought by the disturbance could always be mitigated with the aid of ES.

V. Conclusion

In this paper, a simple decoupling control scheme is proposed for the power flow control of ES in a microgrid with variable and uncertain renewables. The proposed strategy could realize the active power and reactive power control of ES by adjusting the shift angle and the amplitude of the modulation signal. When connected to the load in series, the ES provides the voltage support to prevent the voltage dip on the bus it is installed, and the bus voltage could be tightly regulated at a given deviation during transients. In addition, the frequency nadir could be enhanced for the sake of the active power contributed by ES. Thus the steady-state frequency deviation could be further improved. When ES is installed on the different bus with the disturbance source, the problems concerned with the frequency in the microgrid could still be mitigated effectively. It has been explored that ES could be a potential key component in the future smart grid with substantial renewable energy sources.

Appendix

Nine-Bus System Data
Machine Data:

Parameters	Gen1	Gen2	Gen3
H (secs)	23.64	6.4	3.01
X_d (p.u.)	0.146	0.8958	1.3125
X_d' (p.u.)	0.0608	0.1198	0.1813
X_q (p.u.)	0.0969	0.8645	1.2578
X_q' (p.u.)	0.0969	0.1969	0.25
T_{d0}' (p.u.)	8.96	6.0	5.89
T_{q0}' (p.u.)	0.31	0.535	0.6

Exciter Data for IEEE Type DC1A Excitation Model:

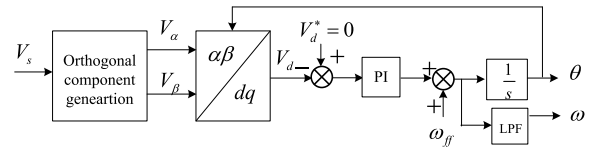| Parameters	Exciter 1	Exciter 2	Exciter 3
K_A	20	20	20
T_A (sec)	0.2	0.2	0.2
K_E	1.0	1.0	1.0
T_E (sec)	0.314	0.314	0.314
K_F	0.063	0.063	0.063
T_F (sec)	0.35	0.35	0.35

ES Parameters:
 Filter inductance: 0.4 mH
 Filter capacitance: 13 μF
 DC link: $C_S = 4000$ μF, $V_{dc} = 40$ kV, and $V_{ac} = 35$ kV
 PWM switching frequency: 1 kHz

Parameters	DC Voltage	AC Voltage
K_p	0.3	0.2
K_i	0.05	0.05

Structure of a Single-Phase PLL:

References

[1] R. H. Lassseter, "Smart distribution: Coupled microgrids," *Proc. IEEE*, vol. 99, no. 6, pp. 1074–1082, Jun. 2011.

[2] A. Camacho, M. Castilla, J. Miret, J. C. Vasquez, and E. Alarcón-Gallo, "Flexible voltage support control for three-phase distributed generation inverters under grid fault," *IEEE Trans. Ind. Electron.*, vol. 60, no. 4, pp. 1429–1439, Apr. 2013.

[3] Y. M. Atwa and E. F. El-Saadany, "Probabilistic approach for optimal allocation of wind based distributed generation in distribution systems," *IET Renew. Power Gener.*, vol. 5, no. 1, pp. 79–88, 2011.

[4] M. Savaghebi, A. Jalilian, J. C. Vasquez, and J. Guerrero, "Secondary control for voltage quality enhancement in microgrids," *IEEE Trans. Smart Grid*, vol. 3, no. 4, pp. 1893–1902, Dec. 2012.

[5] Y. Deng, X. Ren, C. Zhao, and D. Zhao, "A heuristic and algorithmic combined approach for reactive power optimization with time-varying load demand in distribution systems," *IEEE Trans. Power Syst.*, vol. 17, no. 4, pp. 1068–1072, Oct. 2002.

[6] S. Tomonobu, M. Yoshitaka, A. Yona, and F. Toshihisa, "Optimal distribution voltage control and coordination with distributed generation," *IEEE Trans. Power Del.*, vol. 23, no. 2, pp. 842–850, Apr. 2008.

[7] Y. Li and Y. Li, "Power management of inverter interfaced autonomous microgrid based on virtual frequency-voltage frame," *IEEE Trans. Smart Grid*, vol. 2, no. 1, pp. 30–40, Mar. 2011.

[8] L. R. Chang-Chien, W. T. Lin, and Y. C. Yin, "Enhancing frequency response control by DFIGs in the high wind penetrated power systems," *IEEE Trans. Power Syst.*, vol. 26, no. 2, pp. 710–718, May 2011.

[9] J. V. Milanovic, H. Ali, and M. T. Aung, "Influence of distributed wind generation and load composition on voltage sags," *IET Gener. Transmiss. Distrib.*, vol. 1, no. 1, pp. 13–22, Jan. 2007.

[10] H. Hatami, F. Shahnia, A. Pashaei, and S. H. Hosseini, "Investigation on D-STATCOM and DVR operation for voltage control in distribution networks with a new control strategy," in *Proc. IEEE Lausanne Power Tech*, Lausanne, Switzerland, Jul. 2007, pp. 2207–2212.

[11] S. Dasgupta, S. K. Sahoo, S. K. Panda, and G. J. Amaratunga, "Single-phase inverter-control techniques for interfacing renewable energy sources with microgrid—Part II: Series-connected inverter topology to mitigate voltage-related problems along with active power flow control," *IEEE Trans. Power Electron.*, vol. 26, no. 3, pp. 732–746, Mar. 2011.

[12] A. Arulampalam, M. Barnes, N. Jenkins, and J. B. Ekanayake, "Power quality and stability improvement of a wind farm using STATCOM supported with hybrid battery energy storage," *IEE Proc. Gener. Transmiss. Distrib.*, vol. 153, no. 6, pp. 701–710, Nov. 2006.

[13] G. Suvire, M. Molina, and P. Mercado, "Improving the integration of wind power generation into AC microgrids using flywheel energy storage," *IEEE Trans. Smart Grid*, vol. 3, no. 4, pp. 1945–1954, Dec. 2012.

[14] G. Delille, B. Francois, and G. Malarange, "Dynamic frequency control support by energy storage to reduce the impact of wind and solar generation on isolated power system's inertia," *IEEE Trans. Sustain. Energy*, vol. 3, no. 4, pp. 931–939, Oct. 2012.

[15] A. Arulampalamand and T. K. Saha, "Fast and adaptive under frequency load shedding and restoration technique using rate of change of frequency to prevent blackouts," in *Proc. IEEE PES Gen. Meeting*, Minneapolis, MN, USA, Jul. 2010, pp. 1–8.

[16] H. T. Le, S. Santoso, and W. M. Grady, "Development and analysis of an ESS-based application for regulating wind farm power output variation," in *Proc. IEEE PES Gen. Meeting*, Calgary, AB, Canada, Jul. 2009, pp. 1–8.

[17] G. O. Suvire, P. E. Mercado, and L. J. Ontiveros, "Comparative analysis of energy storage technologies to compensate wind power short-term fluctuations," in *Proc. IEEE/PES Transmiss. Distrib. Conf. Expo.*, Sao Paulo, Brazil, Nov. 2010, pp. 522–528.

[18] (2011). *Assessment of Demand Response and Advanced Metering*. [Online]. Available: http://www.ferc.gov/legal/staff-reports/11-07-11-demand-response.pdf

[19] M. Parvania and M. Fotuhi-Firuzabad, "Demand response scheduling by stochastic SCUC," *IEEE Trans. Smart Grid*, vol. 1, no. 1, pp. 89–98, Jun. 2010.

[20] S. Y. R. Hui, C. K. Lee, and F. F. Wu, "Electric springs—A new smart grid technology," *IEEE Trans. Smart Grid*, vol. 3, no. 3, pp. 1552–1561, Sep. 2012.

[21] S. C. Tan, C. K. Lee, and S. Y. R. Hui, "General steady-state analysis and control principle of electric springs with active and reactive power compensations," *IEEE Trans. Power Electron.*, vol. 28, no. 8, pp. 3958–3969, Aug. 2013.

[22] C. K. Lee and S. Y. R. Hui, "Reduction of energy storage requirements for smart grid using electric springs," *IEEE Trans. Smart Grid,* vol. 4, no. 2, pp. 1282–1288, Sep. 2013.

[23] M. Monfared, S. Golestan, and J. M. Guerrero, "Analysis, design, and experimental verification of a synchronous reference frame voltage control for single-phase inverters," *IEEE Trans. Ind. Electron.*, vol. 26, no. 3, pp. 1–11, Dec. 2012.

[24] N. R. Ullah, T. Thiringer, and D. Karlsson, "Temporary primary frequency control support by variable speed wind turbines—Potential and applications," *IEEE Trans. Power Syst.*, vol. 21, no. 3, pp. 601–612, May 2008.

[25] N. W. Miller, W. W. Price, and J. J. Sanchez-Gasca, *Dynamic Modeling of GE 1.5 and 3.6 Wind Turbine Generators*, *Version 3.0*, Gen. Elect. Int., Inc., Schenectady, NY, USA, Oct. 2003.

Xia Chen (M'13) received the B.Eng. degree from the Wuhan University of Technology, Wuhan, China, in 2006, and the M.Eng. and Ph.D. degrees in electrical engineering from the Huazhong University of Science and Technology, Wuhan, in 2008 and 2012, respectively.

She has been a Post-Doctoral Research Fellow with the University of Hong Kong, Hong Kong, since 2012. Her current research interests include large scale power system operation and control, renewable energy integration, and smart grid technologies.

Yunhe Hou (M'08) received the B.E. and Ph.D. degrees in electrical engineering from the Huazhong University of Science and Technology, Wuhan, China, in 1999 and 2005, respectively.

He was a Post-Doctoral Research Fellow at Tsinghua University, Beijing, China, from 2005 to 2007, and a Post-Doctoral Researcher at Iowa State University, Ames, IA, USA, and the University College Dublin, Dublin, Ireland, from 2008 to 2009. He was also a Visiting Scientist at the Laboratory for Information and Decision Systems, Massachusetts Institute of Technology, Cambridge, MA, USA, in 2010. Since 2011, he has been a Joint Professor with the State Key Laboratory of Advanced Electromagnetic Engineering and Technology, Huazhong University of Science and Technology. He joined the faculty of the University of Hong Kong, Hong Kong, in 2009, where he is currently an Assistant Professor with the Department of Electrical and Electronic Engineering.

Siew-Chong Tan (S'00–M'06–SM'11) received the B.Eng. (Hons.) and M.Eng. degrees in electrical and computer engineering from the National University of Singapore, Singapore, in 2000 and 2002, respectively, and the Ph.D. degree in electronic and information engineering from Hong Kong Polytechnic University, Hong Kong, in 2005.

From 2005 to 2012, he was a Research Associate, a Post-Doctoral Fellow, a Lecturer, and an Assistant Professor with the Department of Electronic and Information Engineering, Hong Kong Polytechnic University. In 2009, he was a Visiting Scholar with the Grainger Center for Electric Machinery and Electromechanics, University of Illinois at Urbana-Champaign, Urbana, IL, USA, for one month, and an Invited Academic Visitor at the Huazhong University of Science and Technology, Wuhan, China, in 2011. In 2011, he was a Senior Scientist with the Agency for Science, Technology and Research (A*Star), Singapore, for nine months. He is currently an Associate Professor with the Department of Electrical and Electronic Engineering, University of Hong Kong, Hong Kong. His current research interests include power electronics and control, light emitting diode lightings, smart grids, and clean energy technologies.

Chi-Kwan Lee (M'08–SM'14) received the B.Eng. and Ph.D. degrees in electronic engineering from the City University of Hong Kong, Hong Kong, in 1999 and 2004, respectively.

Since 2012, he has been an Assistant Professor at the Department of Electrical and Electronic Engineering, University of Hong Kong, Hong Kong. He was a Post-Doctoral Research Fellow at the Power and Energy Research Centre, National University of Ireland, Galway, Ireland, from 2004 to 2005. In 2006, he joined the Centre of Power Electronics, City University of Hong Kong, as a Research Fellow. From 2008 to 2011, he was a Lecturer of Electrical Engineering at Hong Kong Polytechnic University, Hong Kong. He was a Visiting Academic at Imperial College London, London, U.K., from 2010 to 2013. His current research interests include applications of power electronics to power systems, advanced inverters for renewable energy and smart grid applications, reactive power control for load management in renewable energy systems, wireless power transfer, energy harvesting, and planar electromagnetics for high frequency power converters.

Shu Yuen Ron Hui (M'87–SM'94–F'03) received the B.Sc. (Hons.) degree in engineering from the University of Birmingham, Birmingham, U.K., in 1984, and the D.I.C. and Ph.D. degrees in electrical and electronics engineering from Imperial College London, London, U.K., in 1987.

He has published over 300 technical papers, including over 180 refereed journal publications and holds 55 patents that have been adopted by industry.

Prof. Hui is the recipient of the IEEE Rudolf Chope Research and Development Award from the IEEE Industrial Electronics Society, the Institution of Engineering and Technology Achievement Medal (the Crompton Medal), and the 2015 William E. Newell Power Electronics Award. He is currently the Philip Wong Wilson Wong Chair Professor with the University of Hong Kong, Hong Kong, and the Chair Professor with Imperial College London. He is an Associate Editor of the IEEE TRANSACTIONS ON POWER ELECTRONICS and the IEEE TRANSACTIONS ON INDUSTRIAL ELECTRONICS, and an Editor of the IEEE JOURNAL OF EMERGING AND SELECTED TOPICS IN POWER ELECTRONICS. He is a Fellow of the Australian Academy of Technological Sciences and Engineering.